Neurobiology of Disease 71 (2014) 180–192

Contents lists available at ScienceDirect

Neurobiology of Disease

journal homepage: www.elsevier.com/locate/ynbdi

Effects of diet-induced obesity and voluntary exercise in a tauopathy mouse model: Implications of persistent hyperleptinemia and enhanced astrocytic leptin receptor expression

Shunsuke Koga [c], Ayako Kojima [a], Chieko Ishikawa [a,b], Satoshi Kuwabara [c], Kimihito Arai [b,c], Yasumasa Yoshiyama [a,b,c,*]

[a] Laboratory for Neurodegenerative Disorder Research, Clinical Research Center, Chiba-East National Hospital, Japan
[b] Department of Neurology, Chiba-East National Hospital, Japan
[c] Department of Neurology, School of Graduate Medicine, Chiba University, Japan

ARTICLE INFO

Article history:
Received 14 January 2014
Revised 2 August 2014
Accepted 10 August 2014
Available online 15 August 2014

Keywords:
Obesity
Leptin
Tau
Astrocyte
Neuroinflammation

ABSTRACT

The number of patients with Alzheimer's disease (AD) is increasing worldwide, and available drugs have shown limited efficacy. Hence, preventive interventions and treatments for presymptomatic AD are currently considered very important. Obesity rates have also been increasing dramatically and it is an independent risk factor of AD. Therefore, for the prevention of AD, it is important to elucidate the pathomechanism between obesity and AD. We generated high calorie diet (HCD)-induced obese tauopathy model mice (PS19), which showed hyperleptinemia but limited insulin resistance. HCD enhanced tau pathology and glial activation. Conversely, voluntary exercise with a running wheel normalized the serum leptin concentration without reducing body weight, and restored the pathological changes induced by HCD. Thus, we speculated that persistent hyperleptinemia played an important role in accelerating pathological changes in PS19 mice. Leptin primarily regulates food intake and body weight via leptin receptor b (LepRb). Interestingly, the nuclear staining for p-STAT3, which was activated by LepRb, was decreased in hippocampal neurons in HCD PS19 mice, indicating leptin resistance. Meanwhile, astroglial activation and the astrocytic expression of a short LepR isoform, LepRa, were enhanced in the hippocampus of HCD PS19 mice. Real-time PCR analysis demonstrated that leptin increased mRNA levels for pro-inflammatory cytokines including IL-1β and TNF-α in primary cultured astrocytes from wild type and LepRb-deficient mice. These observations suggest that persistent hyperleptinemia caused by obesity induces astrocytic activation, astrocytic leptin hypersensitivity with enhanced LepRa expression, and enhanced inflammation, consequently accelerating tau pathology in PS19 mice.

Introduction

The rapid increase in the size of the elderly population has resulted in a dramatic increase in the number of patients with dementia. Of all diseases causing dementia, Alzheimer's disease (AD) is the most prevalent, contributing up to 60–70% of all dementia cases. Current therapies for AD only provide symptomatic relief, either by temporarily improving symptoms above baseline or by delaying cognitive decline. Thus, disease-modifying therapies based on the pathomechanisms of AD are a central focus of AD drug discovery. Although the pathomechanisms of AD are still unclear, β-amyloid protein (Aβ) and tau protein are common targets for disease-modifying therapies. However, recent clinical trials based on the amyloid hypothesis and aiming to reduce the production of Aβ or to remove the accumulated Aβ from the brain have failed to demonstrate significant clinical efficacy, although the hope that these therapies will have some beneficial effects has not been completely abandoned. Additionally, tau-targeting therapies have also failed to yield results for the treatment of AD and related tauopathies, although tau pathology is thought to be more directly related to neurodegeneration and cognitive decline than Aβ pathology (Yoshiyama et al., 2013). Along with these clinical observations, disease-modifying therapies have shown limited efficacy towards improving symptomatic AD patients. Therefore, to prevent the onset of clinical symptoms of AD, researchers have turned their attention to the relationship between lifestyle and AD. Lifestyle-related diseases are potentially preventable, and can be decreased with adequate changes in diet, physical activity, and environment without incurring excessive expense. The common feature at the core of most lifestyle diseases is obesity, rates of which have dramatically increased. Worldwide, age-standardized prevalence of obesity was estimated to be 9.8% in men and 13.8% in woman in 2008, and the highest

* Corresponding author at: 679 Nitona, Chuo-ku, Chiba, Chiba 260, Japan. Fax: +81 43 268 2613.
E-mail address: neuroyy@cehpnet.com (Y. Yoshiyama).
Available online on ScienceDirect (www.sciencedirect.com).

http://dx.doi.org/10.1016/j.nbd.2014.08.015

prevalence of obesity was 29.2% in North American men (Finucane et al., 2011). Although it is well-known that obesity is an independent risk factor of AD (Kivipelto et al., 2005; Whitmer et al., 2007; Gustafson et al., 2009; Li et al., 2010; Profenno et al., 2010), obesity induces other AD risk factors. It is therefore difficult to clarify the effects obesity itself and its mechanisms have on AD while excluding other contributing factors and complications related to obesity (such as diabetes mellitus) in human research. Thus, it is important to generate appropriate models to evaluate the pathological relationship between obesity and AD.

High calorie diets (HCD) used in a majority of diet-induced obesity studies usually contain around 550 cal/100 g, and typically induce glucose metabolism abnormalities and insulin resistance (diabetes mellitus). To develop an obese tauopathy mouse model with fewer complicating factors induced by obesity, we used a moderately high calorie diet containing 415 cal/100 g. This allowed us to develop an obese tauopathy mouse model that showed obvious hyperleptinemia but limited insulin resistance. Interestingly, both tau pathology and glial activation were enhanced in these mice, and the expression of certain isoforms of leptin receptor (LepR) was enhanced in astrocytes. Meanwhile, voluntary exercise (EX) with a running wheel reduced hyperleptinemia without altering body weight, and also reduced the tau pathology and glial activation. These findings suggest that the persistent hyperleptinemia might be an important factor that enhances tau pathology.

Methods

Animals

The generation of transgenic (Tg) mice carrying the human tau gene harboring a P301S mutation was previously described by our group (Yoshiyama et al., 2007). Briefly, a cDNA construct of human tau isoform T34 (1N4R) harboring the P301S mutation was cloned into the MoPrP.Xho expression vector containing a mouse prion (MoPrP) promoter (Borchelt et al., 1996) at the XhoI site. A 15-kb NotI fragment containing T34 and the MoPrP promoter together with 39 bp of untranslated sequence was used as the transgene to create tau Tg mice in a B6C3H/F1 background. A stable Tg line (PS19) and non-Tg offspring were identified by PCR analysis of tail genomic DNA.

To reduce potential variations in tau pathology, body weight and metabolism, we used only female mice. Female PS19 mice were exposed to either HCD [15.3% fat (source: beef tallow; composition: saturated, 41%; monosaturated, 44%; polysaturated, 10%: oleic acid, 40%; palmitic acid, 24%; stearic acid, 14%; linoleic acid (n-6), 9%; linolenic acid (n-3), 1%), 415 cal/100 g, Quick Fat (Clea Japan Inc., Japan)] or standard rodent laboratory diet (SD) (4.5 % fat, 330 cal/100 g, Lab Diet 5 L65, Japan SLC, Inc., Japan) from 1.5 to 10 months of age.

The animals in the HCD group were housed in either a regular cage or a cage equipped with a running wheel (CL-4579-2. Clea Japan, Inc., Japan) (from 1.5 to 10 months of age). The average amount of exercise was $9.0 \pm 2.0 \times 10^3$ rounds/day ($\approx 5.6 \pm 1.2$ km/day, mean $\pm$ SD). At 10 months of age, animals were decapitated, and blood (500–700 μl) was collected from the left ventricle of the heart for analysis. Serum samples were stored at −80 °C until measurements. Brain specimens were harvested and hemi-dissected: One hemisphere was microdissected and the other was postfixed in 4% PFA. All tissues used for biochemical analysis were stored at −80 °C, whereas tissue processed for immunohistochemistry was stored at 4 °C. There was no difference in survival among any of the groups. The final numbers of subjects in the SD, HCD, and HCD + EX groups for this study were 13, 12, and 10, respectively.

All experiments were approved by the Committee of Animal Care and Control in Chiba East National Hospital.

Assessment of metabolic changes

Body weight was recorded every 4 weeks throughout the study. Fasting serum insulin and leptin levels were determined using the enzyme-linked immunosorbent assay (ELISA) kit (Morinaga Institute of Science, Inc., Japan). Fasting serum total cholesterol level was determined using a colorimetric assay performed with commercial reagents (BioVision, Inc., San Francisco, CA, USA). Fasting serum triglyceride level was determined using Accutrend GCT (Roche Diagnostics, Switzerland). Intraperitoneal glucose tolerance tests (IGTT) were performed in PS19 mice (SD, n = 12; HCD, n = 13; HCD + EX, n = 6) one week before sacrifice. On the night before the IGTTs, food was removed at 6:00 PM, and at 9 AM the next day, and mice were given a single-dose intraperitoneal injection of glucose (2 g/kg body weight) (15 hours fasting). Blood samples were collected from the tail vein immediately before glucose administration and again at 15, 30, 60, and 120 min post-gavage. Blood glucose was assessed using Glutest Ace R (Sanwa Kagaku Kenkyusho Co., Ltd., Japan) following the manufacturer's instructions. Insulin tolerance tests (ITTs) were performed in PS19 mice (SD, n = 10; HCD, n = 12; HCD + EX, n = 6) two weeks before sacrifice. The mice were intraperitoneally injected with insulin (0.75 U/kg diluted in 0.1 ml of 0.9% NaCl). Blood samples were collected from the tail vein immediately before the injection of insulin and again at 15, 30, 45, 60, and 120 min after the insulin injection. Blood glucose was assessed by using Glutest Ace R.

Tau insolubility and phosphorylation states

Proteins were extracted by solubilizing brain tissue in radioimmunoprecipitation assay (RIPA) buffer [50 mM Tris, 150 mM NaCl, 0.1% SDS, 0.5% sodium deoxycholate, 1% NP40, 5 mM EDTA, and protease inhibitor cocktail (protease inhibitor cocktail set I (Calbiochem, Merck, Germany); final pH 8.0)], using 1 ml/g. Samples were then centrifuged at 40,000 *g* for 40 min at 4 °C. The supernatants were used as RIPA-soluble samples, while the RIPA-insoluble pellets were extracted using 70% formic acid (FA) to recover highly insoluble protein.

Imaging and statistical analyses

Images were captured with a Nikon Eclipse 80i microscope and a Nikon DXM 1200C digital camera, and analyzed using ImageJ software (National Institutes of Health, Bethesda, MD). The results were expressed as the mean ± SE. Statistically significant differences were determined by analysis of variance using SPSS statistical software (SPSS, Chicago, IL, USA). Statistical significance was set at $P < 0.05$.

Western blot analysis

Protein concentrations of RIPA-extracted samples were determined using a BCA protein assay kit (Pierce, Rockford, IL), and proteins were resolved by SDS-PAGE, followed by western blotting. Signals were detected by enhanced chemiluminescence (GE Healthcare, WI, USA) according to the manufacturer's instructions. The antibodies and corresponding dilutions used are listed in Table 1.

Primary cortical astrocyte cultures

Enriched cultures of astrocytes were generated using the method developed by McCarthy and de Vellis (1980). First, mixed glia cultures were generated from 1- to 2-day-old mice. Mouse brains were aseptically removed and placed in sterile culture dishes containing Hank's balanced salt solution. The meninges and blood vessels were removed by dissection, and the cerebral cortices (including the hippocampus) were isolated from the brain. The cerebral cortices were mechanically dissociated and suspended in Dulbecco's Modified Eagle Medium (DMEM) supplemented with 10% fetal bovine serum, 7.5 mM glucose, 4 mM L-glutamine, 1000 U/ml penicillin, and 1 ng/ml streptomycin. Next, cells were centrifuged at 2000 rpm for 5 min, resuspended in 10% DMEM, and placed in 75-cm^2 flask. Cultures were maintained in 10% DMEM at 37 °C in an atmosphere of 5% CO_2. After one week, cells were mechanically dissociated

Table 1
Primary antibodies used in this study.

Antibody	Immunogen	Host	Dilution for IHC	Dilution for WB	Source
17026	Total tau	Rabbit		×1000	Ishihara et al., 1999
T181	Anti-phospho-Tau (pThr181)	Rabbit		×1000	Sigma (Sigma-Aldrich, MO)
Syntaxin	Synaptic vesicle containing fractions of immunoprecipitated human brain homogenate	Mouse	×500		Santa Cruz Biotechnology (Santa Cruz, CA)
Iba1	C terminus of Iba1	Rabbit	×1000		Wako (Osaka, Japan)
SAPK/JNK	Human JNK2	Rabbit		×1000	Cell Signaling (Beberly, MA)
p-SAPK/JNK	Phosphopeptide surrounding Thr183/Tyr185 of human SAPK/JNK	Rabbit		×1000	Cell Signaling (Beberly, MA)
GSK-3β	aa 345–420 of human GSK-3β	Rabbit		×500	Santa Cruz Biotechnology (Santa Cruz, CA)
p-GSK-3β	aa containing phosphorylated ser9 of human GSK-3β	Goat		×500	Santa Cruz Biotechnology (Santa Cruz, CA)
CDK5	aa 1–291 of human cdk5	Mouse		×500	Santa Cruz Biotechnology (Santa Cruz, CA)
p-CDK5	aa containing phosphorylated Ser159 of human cdk5	Goat		×500	Santa Cruz Biotechnology (Santa Cruz, CA)
p38 MAPK	aa corresponding to residues near the carboxy terminus of human p38 protein.	Rabbit		×1000	Cell Signaling (Beberly, MA)
p-p38MAPK	Phosphopeptides surrounding Thr180/Tyr182 of human p38	Rabbit		×1000	Cell Signaling (Beberly, MA)
p-p38MAPK	Phosphopeptides surrounding Thr180/Tyr182 of human p38	Mouse		×1000	Cell Signaling (Beberly, MA)
ERK1/2	aa corresponding to residues near the C-terminus of rat p44 MAP kinase	Rabbit		×1000	Cell Signaling (Beberly, MA)
p-ERK1/2	aa corresponding to residues near the C-terminus of rat p44 MAP kinase	Rabbit		×1000	Cell Signaling (Beberly, MA)
α-tubulin	aa 426–430 of alpha-tubulin	Mouse		×1000	Sigma (Sigma-Aldrich, MO)
M18	aa 877–894 of leptin receptor, highest for leptin receptor a, less for leptin receptor c and d	Goat	×100		Santa Cruz Biotechnology (Santa Cruz, CA)
K20	N-terminal of leptin receptor (all isoforms)	Chicken	×100		Santa Cruz Biotechnology (Santa Cruz, CA)
CH14014	Leptin receptor b	Chicken	×100		Neuromics Antibody (Neuromics, MN)
pAKT	p-Akt1/2/3 (Ser 473)	Rabbit		×500	Santa Cruz Biotechnology (Santa Cruz, CA)
pSTAT3	phosphorylated STAT3 at Tyr705	Rabbit	×100		Cell Signaling (Beberly, MA)
AMPK	N-terminal sequence of human AMPKα	Rabbit		×1000	Cell Signaling (Beberly, MA)
pAMPK	Phospho-AMPKα (Thr172)	Rabbit		×1000	Cell Signaling (Beberly, MA)
GFAP	Recombinant GFAP	Chicken	×1000		Neuromics Antibody (Neuromics, MN)

IHC, immunohistochemistory; WB, western blotting.

to generate cultures enriched for astrocytes (>98%). Astrocytes were harvested by trypsinization, plated in 3.5 cm dishes, and maintained in 10% DMEM for one day to reach almost 80% confluency. One day prior to experiments, cultures were switched to full DMEM. For the leptin load experiment, astrocytes were incubated in 10% DMEM plus varying concentrations of leptin for one day.

RT-PCR analysis of mRNA of leptin receptor subtypes in cultured mouse astrocytes

Total RNA was extracted using an RNeasy Plus Mini Kit (Qiagen, Venlo, Netherlands), and first-strand cDNA was synthesized using SuperScript VILO cDNA synthesis kit (Invitrogen, Carlsbad, CA, USA). The PCR condition for LepRa was as follows: denaturation at 95 °C for 5 min, followed by 35 cycles of denaturation at 95 °C for 1 min, annealing at 55 °C for 1 min, and extension at 72 °C for 1 min. PCR conditions for other LepR isoforms used the same conditions, except for the annealing temperature (LepRb at 59 °C, LepRc at 54 °C, LepRd at 48 °C and LepRe at 54 °C). The primer sequences were generated by Hsuchou et al. (2009).

Real-time PCR

The mRNA levels of IL-1β, CCL2 and TNF-α transcripts were analyzed by quantitative real-time PCR using the ABI PRISM® 7900HT sequence detection system (Applied Biosystems, Foster City, CA, USA). PCR reactions consisted of 2.5 μl of TaqMan® Universal Master Mix II, no UNG, 0.25 μl of TaqMan® Gene EXpression Assay, 1.75 μl of UltraPure™ distilled water, and 0.5 μM cDNA. PCR cycling was as follows: 10 min at 95 °C, followed by 40 cycles of 95 °C for 15 s and 60 °C for 1 min. Samples were run in triplicate. β-Actin was used as the endogenous reference transcript. The results of the PCR reactions were analyzed by ABI PRISM SDS 2.1 software.

Results

HCD induces obesity and hyperleptinemia, but limited insulin resistance in PS19 mice; EX reduces hyperleptinemia without reducing body weight

PS19 mice fed HCD showed a significant increase in the body weight from 4 months to the experimental endpoint (10 months), and around 20% body weight gain was observed after 5 months compared with mice fed SD. HCD + EX PS19 mice did not show any significant reduction in body weight compared with the HCD PS19 mice, and the change in body weight with age was almost identical in these two groups (Fig. 1A). This indicated that metabolic and pathological changes in the EX group were not due to a reduction in the fat volume. The average fasting serum insulin levels in the HCD group seemed elevated, but were not statistically significant (Fig. 1B), and there was no significant difference in the levels of fasting blood glucose (Fig. 1C). The IGTT showed a mild elevation in blood glucose at 15, 60, and 120 min, and representative areas under the curve (AUC) were higher in HCD than in SD. HCD + EX showed a slight elevation in blood glucose only at 120 min, but no difference in AUC (Fig. 1C), whereas in the ITT there was no difference in the peak rate of lowering blood glucose (SD at 30 min, HCD and HCD + EX at 45 min). Additionally, AUC showed no differences in each group, although the declining rate of lowering blood glucose after insulin injection was slower in HCD (Fig. 1D). Moreover, western blotting of brain homogenate samples for pAKT, a downstream target of insulin signaling, showed no significant difference in each group (Fig. 1D). These data indicated that the glucose metabolic abnormality seemed to be mild, and there was limited insulin resistance. Meanwhile, the serum leptin level in HCD was significantly elevated. EX normalized the level, indicating that HCD-induced leptin resistance was recovered in EX (Fig. 1E). In SD, because of a little dispersion in BW and serum leptin concentrations (Figs. 1A, E), the correlation between BW and leptin was ambiguous ($y = 0.067x + 0.93$, $R^2 = 0.024$, $p = 0.94$). However, in HCD and HCD + EX, there were significant proportionate correlations (HCD, $y = 1.1x + 22.5$, $R^2 = 0.75$, $p < 0.01$; HCD + EX, $y = 0.43x + 10.6$,

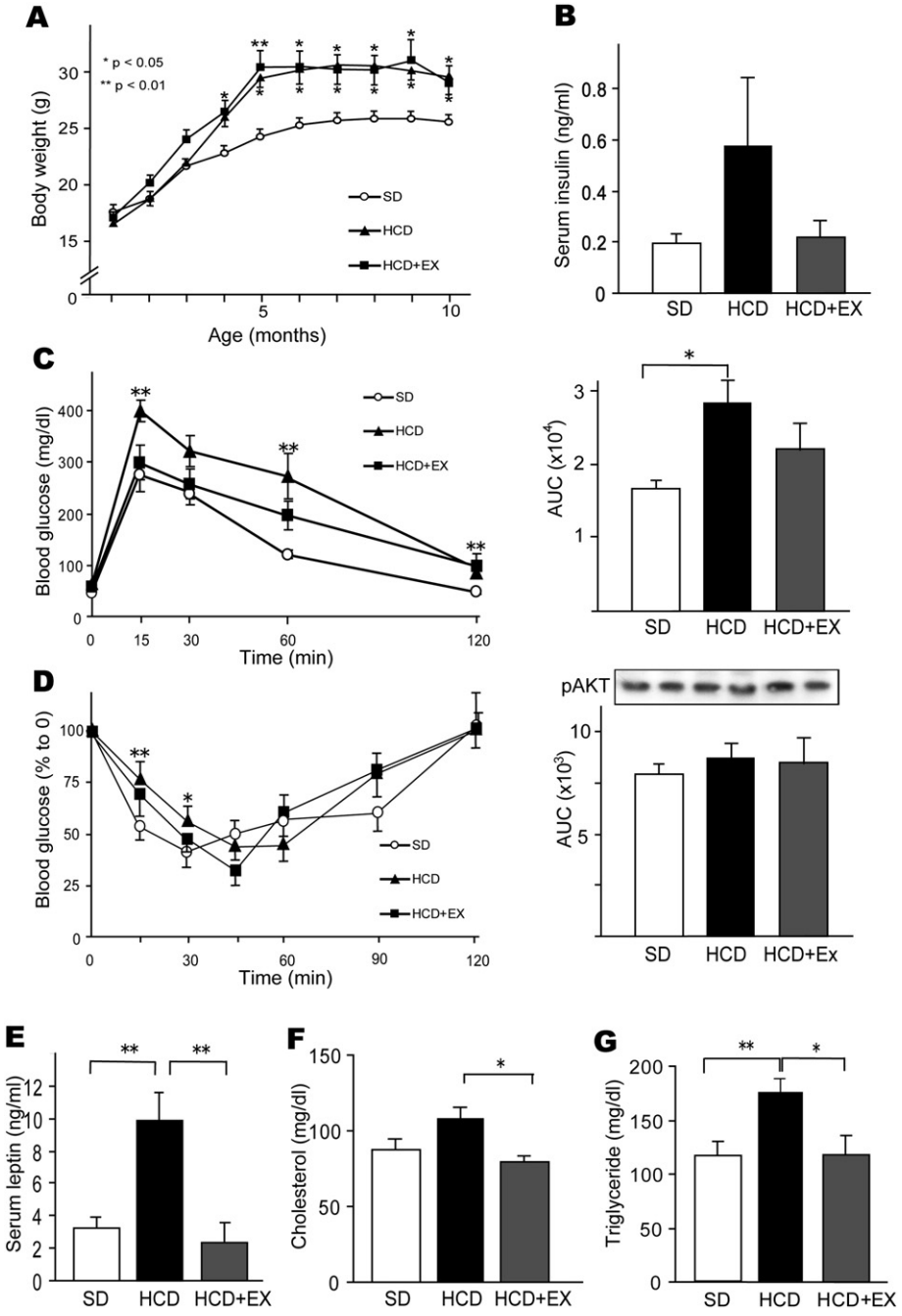

Fig. 1. High calorie diet (HCD) induces obesity and hyperleptinemia, but not insulin resistance; voluntary exercise (EX) restores those abnormalities. The average body weight in PS19 mice fed the HCD is significantly increased compared with PS19 mice fed the standard chow diet (SD). Meanwhile, EX with a running wheel does not decrease the average body weight (A). Although the average insulin level is higher in HCD, it is not significant (B). Intraperitoneal glucose tolerance tests (IGTT) show mild elevated blood glucose levels in HCD-fed PS19 mice at 15, 60 and 120 min, although the fasting glucose levels in each group are identical (n = 13 (SD), 12 (HCD), 6 (HCD + EX)). Areas under the curve (AUC) of IGTT in HCD are greater than SD (C) (n = 12 (SD), 10 (HCD), 6 (HCD + EX)). Meanwhile, insulin tolerance tests demonstrated no difference in AUC and the peak rate of lowering blood glucose in each group, although slightly higher blood glucose levels at 15 and 30 min are seen in HCD (D). Moreover, western blotting of brain homogenate samples for pAKT, a downstream target of insulin signaling, showed no significant difference in each group (panel D) indicating that the glucose metabolic abnormality seemed to be mild, and there was limited insulin resistance. Serum leptin is about three times higher in HCD than SD, but EX completely abrogates the change (E). Total cholesterol and triglyceride levels are slightly elevated in HCD (F, G). n = 13 (SD), 12 (HCD), 10 (HCD + EX) (except IGTT, ITT). *, $p < 0.05$; **, $p < 0.01$ to SD; error bars, 1 SE.

$R^2 = 0.81$, $p < 0.01$), and the gradients of linear approximation were significantly higher in HCD than in HCD + EX ($p < 0.01$), indicating EX improved leptin sensitivity.

Cholesterol and triglyceride were mildly elevated in HCD, but returned to normal in EX (Figs. 1F, G). This data on metabolic changes indicated that HCD induced obesity, hyperleptinemia, and mild glucose metabolism abnormalities, but limited insulin resistance, and EX completely reversed the observed hyperleptinemia.

HCD enhances tau pathology and tau insolubility, and EX suppresses tau enhancements

To compare the tau pathology among the groups, brain sections were immunostained with AT8, an antibody specific for phosphorylated tau (Figs. 2A–H). WT mice did not show any AT8-positive staining in the CA1 (Fig. 2D) or CA3 (Fig. 2H) regions. Although the distribution of tau-positive neurons, which were mainly located in the hippocampus,

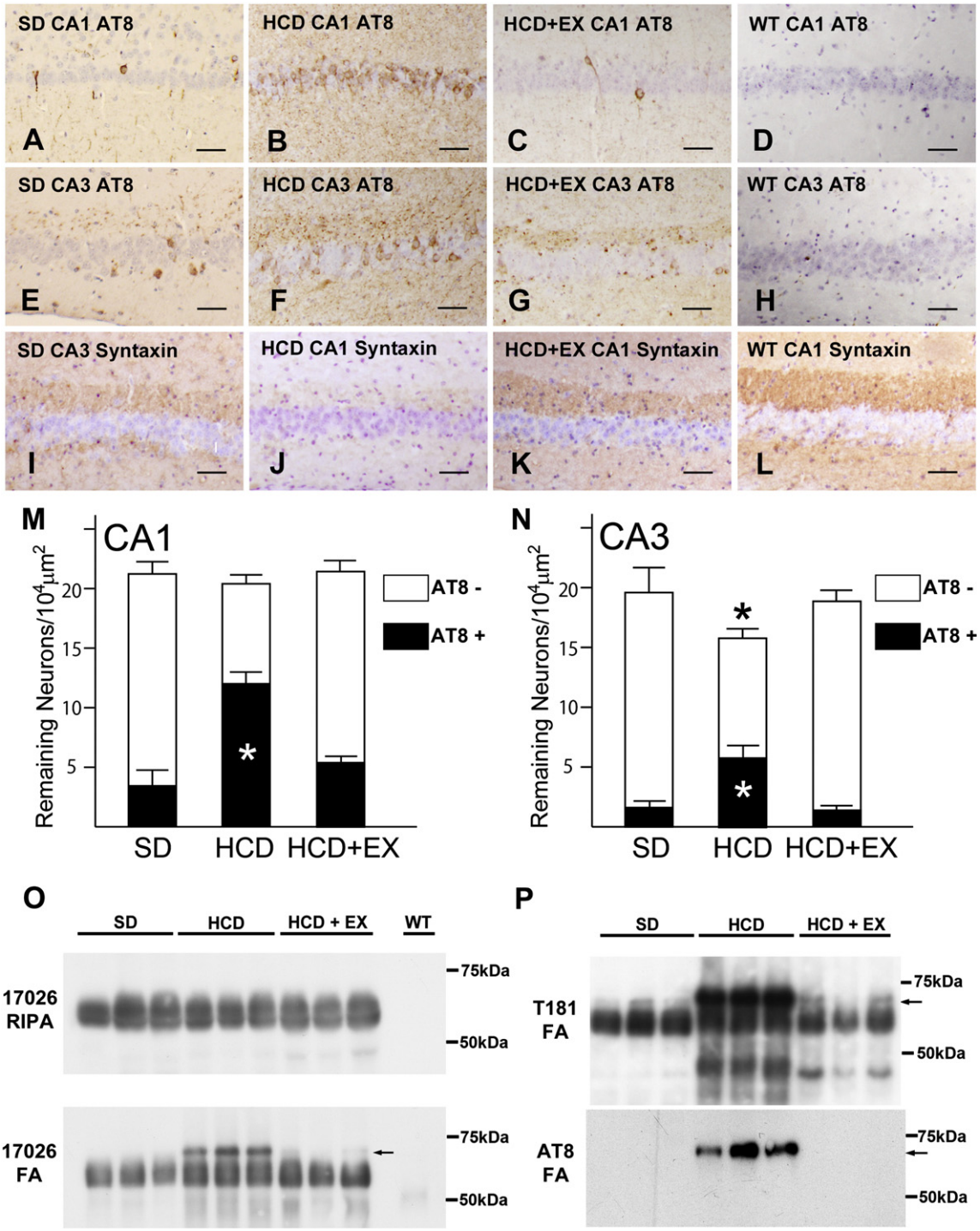

Fig. 2. HCD enhances, but EX mitigates tau pathology and synaptic degeneration. Immunohistochemistry of AT8 antibody (A–H), specific for phosphorylated tau protein, reveals enhanced tau pathology in HCD PS19 mice (B, F) compared with SD PS19 mice (A, E), and HCD + EX PS19 mice show milder tau pathology (C, G) compared with HCD PS19 mice. There is no AT8 staining in WT (D, H). Statistical analysis (n = 4, each group) indicated that in the CA1 region, the number of AT8-positive neurons (black bar) was increased in HCD PS19 mice compared to SD PS19 mice, although the total neuron number was unchanged (M); however, in the CA3 region, the number of AT8-positive neurons (black bar) was mildly increased in HCD PS19 mice. The neuronal loss was significant in HCD mice (N). Syntaxin staining in PS19 mice shows synaptic degeneration in the CA3 region (I, compare with WT (L)). HCD reduces syntaxin staining more (J), whereas syntaxin staining in HCD + EX PS19 mice (K) is similar to the SD PS19 mice (I). Proteins were extracted from mouse brains after mixing with RIPA buffer (50 mM Tris, 150 mM NaCl, 0.1% SDS, 0.5% sodium deoxycholate, 1% NP40, 5 mM EDTA; pH 8.0, and protease inhibitor cocktail) and centrifuging at 50,000 ×*g* for 40 min at 4 °C in an ultracentrifuge. The supernatants were used as RIPA-soluble samples (O, upper panel), and the RIPA-insoluble pellets were extracted with 70% formic acid (FA) to recover highly insoluble protein (O, lower panel; P). Although HCD + EX shows no change in the expression levels of tau protein in the RIPA-soluble samples (O, upper panel) probed with a 17026 polyclonal tau antibody, RIPA-insoluble tau (O, lower panel) is increased in the HCD PS19 mouse brains. Slow-migrating bands (O, lower panel, arrow) are clearly seen and are strongly detected by p-tau specific antibodies T181 (P, upper panel, arrow) and AT8 (P, lower panel, arrow) in the HCD group, indicating that a highly-phosphorylated form of the insoluble-tau protein is markedly increased in the HCD PS19 mouse brains. Scale bars, 50 μm. *, $p < 0.05$, to SD; error bars, 1 SE; n = 4/group.

amygdala, brain stem, and spinal cord, was similar in each group, the HCD PS19 mice showed much stronger tau pathology in the CA1 (Fig. 2B) and CA3 (Fig. 2F) regions compared with the SD PS19 mice (Figs. 2A, E). The HCD + EX PS19 mice exhibited a milder tau pathology than did the HCD PS19 mice (Figs. 2C, G). Statistical analysis (n = 4, each group) also demonstrated enhanced tau pathology in CA1 and CA3, and mild

neuronal loss in CA3 in HCD PS19 mice (Figs. 2M, N). Because synaptic degeneration is one of the earliest pathological changes in PS19 mice (Yoshiyama et al., 2007), we compared synaptic loss in the CA3 region using immunohistochemistry for syntaxin, which stains presynaptic terminals (Figs. 2I–L). Syntaxin staining was intense in the synapse-rich granular layer of CA3 in 10-month-old non-transgenic wild type (WT) mice (Fig. 2L), but was decreased in SD PS19 (Fig. 2I) and HCD + EX PS19 mice (Fig. 2K). Staining was almost completely abolished in HCD PS19 mice (Fig. 2J). This indicated that HCD accelerated synaptic degeneration, and the addition of EX suppressed it.

Because more tau-positive neurons were observed in HCD, the brain tissue from mice was subsequently analyzed for RIPA-soluble and RIPA-insoluble tau. The expression levels of RIPA-soluble tau were almost identical in each group (Fig. 2O, upper panel). However, RIPA-insoluble tau was increased in HCD (Fig. 2O, lower panel). In particular, a slowly migrating band (Fig. 2O, lower panel, arrow), which was highly phosphorylated and specifically recognized by AT8 (Fig. 2P, lower panel), was intense in HCD PS19 mouse brain samples in the RIPA-insoluble fraction. Western blotting with another phosphorylated tau-specific antibody, T181, demonstrated that tau in the RIPA-insoluble fractions was also hyperphosphorylated in HCD PS19 mice (Fig. 2P, upper panel). Interestingly, T181 recognized lower molecular bands strongly, suggesting that the RIPA-insoluble fraction might contain T181-positive truncated or degraded tau proteins.

HCD activates p38 and CDK5, but EX suppresses JNK, p38, and CDK5

Immunohistochemical and biochemical studies indicated that EX attenuated the insolubility and hyperphosphorylation of tau caused by HCD. To elucidate biological alternations in tau, we examined several putative tau kinases and other related kinases (Fig. 3). Specifically, the activated and inactivated forms of GSK-3β, CDK5, and MAPKs were analyzed. Activity of these enzymes is controlled by phosphorylation state, and although most of these enzymes are activated by phosphorylation, GSK3β is inactivated by phosphorylation. In WT mice and in SD, HCD, and HCD + EX PS19 mice, expression of enzymes was similar in all groups, which suggested that basic expression levels of these enzymes were not affected by the transgene, HCD, or EX. HCD showed enhanced enzyme activity for p38 and CDK5, and EX suppressed this effect. JNK activity was clearly suppressed by EX, although it was not clear if HCD enhanced JNK activity. Interestingly, EX did not suppress JNK activity in SD-fed PS19 mice (Supplemental Fig. 1F). In addition to phosphorylating tau, JNK regulates a wide spectrum of intracellular signaling pathways (Chen, 2012), and is involved in metabolic regulation (Hirosumi et al., 2002). Suppression of JNK activation by EX might be related to the corrective effect of EX on the deregulation of metabolism caused by obesity.

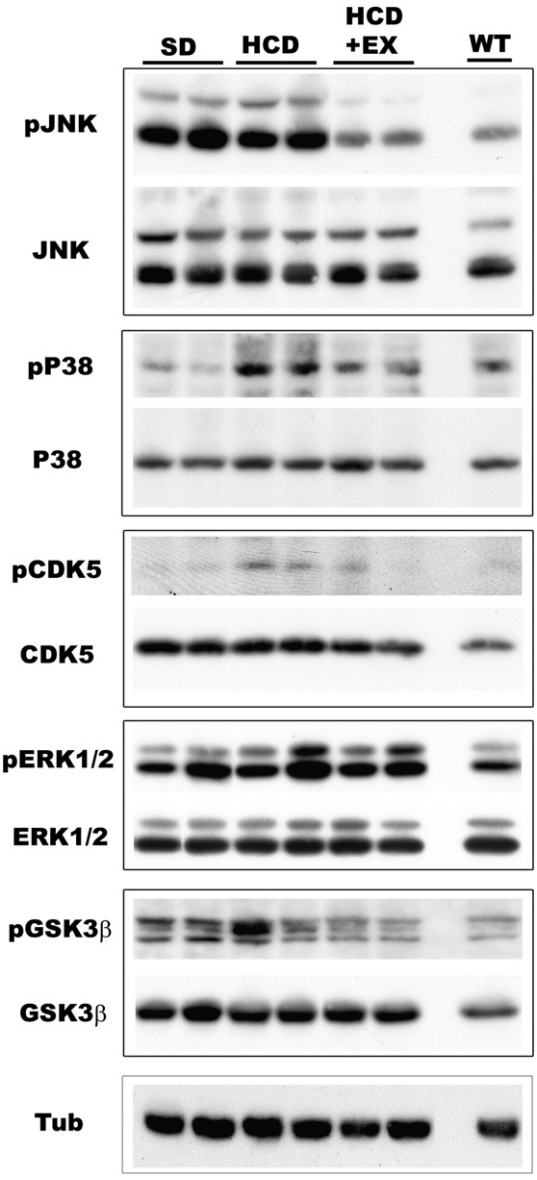

Fig. 3. HCD activates tau kinases, but EX attenuates the activation. To assess the kinase activities involved in tau phosphorylation, western blot analysis was performed for active and inactive kinases, including GSK3β, CDK5 and MAPKs (p38, JNK, ERK), in PS19 brain samples from WT and from SD, HCD and HCD + EX mice. For all enzymes except GSK3β, the phosphorylated (p-) form is the activated form; p-GSK3 is the inactivated form. HCD clearly enhanced the activation of p38, and CDK5, but not JNK, ERK or GSK3β. EX suppresses p38, CDK5, and JNK.

HCD enhances glial activation, but EX suppresses this effect

Microglial-mediated neuroinflammation plays an important role in neurodegeneration in a number of diseases, including tauopathies (Akiyama et al., 2000). In fact, PS19 mice show microglial activation preceding tau pathology and neuronal loss (Yoshiyama et al., 2007). Many studies have indicated that obesity is linked to a state of chronic, low-grade inflammation (Hotamisligil and Erbay, 2008; McArdle et al., 2013; van Greevenbroek et al., 2013), and exercise is known to produce anti-inflammatory effects (Petersen and Pedersen, 2005; Gleeson et al., 2011). Thus, we estimated microglial activation by using two microglia-specific antibodies, Iba1 (Figs. 4A–L) and CD68 (Figs. 4M–O). Immunohistochemistry for Iba1 in hippocampal regions CA1 (Figs. 4A, D, G, J), CA3 (Figs. 4C, F, I, L), and CA4 (Figs. 4B, E, H, K) demonstrated pronounced microglial activation in HCD PS19 mice (Figs. 4D–F) compared to SD PS19 mice (Figs. 4A–C) and WT mice (Figs. 4J–L). Meanwhile, EX suppressed HCD-related microglial activation (Figs. 4G–I). Higher magnification images revealed enlarged, strongly Iba1-positive microglia with thick processes in HCD PS19 mice (Figs. 4D–E, insets), whereas a few small, faintly Iba1-positive microglia with thin processes were observed in the WT mice (Figs. 4J–L, insets). Microglial activation was mainly observed in the hippocampus, amygdala, entorhinal cortex, and brain stem, and corresponded predominantly to regions where tau pathology was observed (data not shown). Because CD68-positive microglia mainly appeared in the granular neuronal layer of the hippocampus that exhibited neuronal loss in older PS19 mice (Yoshiyama et al., 2012), we stained hippocampal sections for CD68. More CD68-positive microglia were seen in the CA3 region of HCD mice (Fig. 4N) compared with those of SD mice (Fig. 4M) or HCD + EX mice (Fig. 4O).

Astrocytes are also involved in the neuroinflammatory process in the brain (Li et al., 2011), and their activation is closely related to the area of neurodegeneration (Fukutani et al., 2000). Astrogliosis was observed in the area exhibiting tau pathology in the PS19 mouse brain (Yoshiyama et al., 2007), and the distribution of astrogliosis closely paralleled that

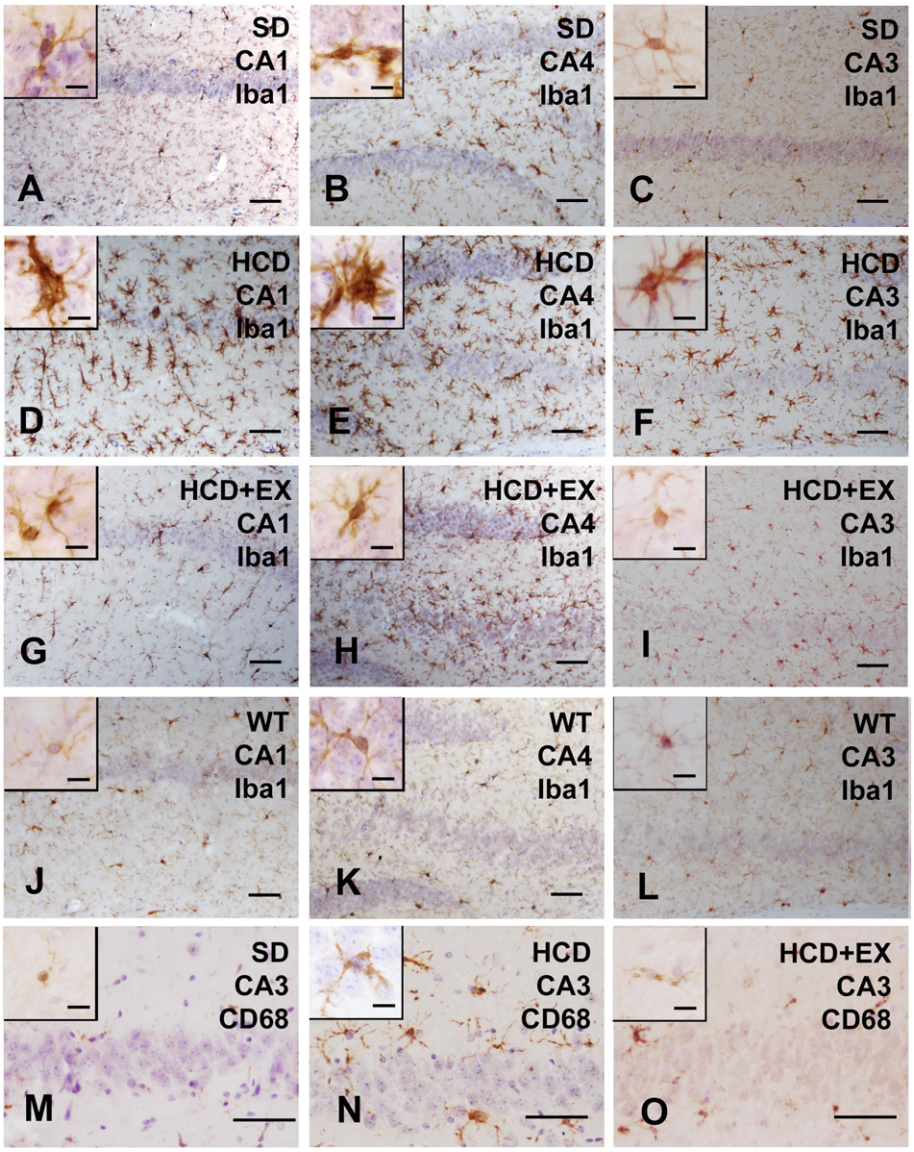

Fig. 4. HCD induces microglial activation, but EX suppresses it. Hippocampal sections (CA1 region, A, D, G, J; CA4 region, B, E, H, K; CA3 region, C, F, I, L, M–O) from SD (A–C, M), HCD (D–F, N) and HCD + EX PS19 mice (G–I, O), and SD WT mice (J–L) were stained with microglia-specific antibodies Iba1 (A–L) and CD68 (M–O). HCD enhances microglial activation, whereas EX reduces that microglial activation. Higher magnification images (insets) indicate morphological changes: enlarged cytoplasm with shorter thick processes. Scale bars, 50 μm; 10 μm in insets.

of microglial activation (Yoshiyama et al., 2010). Astroglial activation was enhanced in the hippocampal region in HCD mice (Fig. 6D), but was suppressed in HCD + EX mice (Fig. 6G). The quantitative analysis of the number of glial fibrillary acidic protein (GFAP)-positive astrocytes in the CA3 (Fig. 6J) and dentate gyrus (Fig. 6K) hippocampal regions indicated that HCD induced more astrogliosis, and that EX attenuated this effect (Figs. 6J, K).

A short isoform of leptin receptor, LepRa, is strongly expressed in activated astrocytes

In this study, HCD-induced obesity induced hyperleptinemia that was attenuated by EX without a reduction in body weight. We hypothesized that hyperleptinemia might play an important role in enhancing tau pathology and glial activation. This prompted us to investigate the

Fig. 5. Leptin receptor a (LepRa) highly expresses in active astrocytes and corresponds to the tau pathology distribution. Low magnification images of brain tissue stained with M18 antibody, which highly recognizes the leptin receptor a (LepRa) and not LepRb, demonstrate clear enhanced staining in the hippocampus from HCD (B), compared with SD (A) and HCD + EX (C). Similarly, the entorhinal cortex (D) and the amygdala (E), where tau accumulation is preferentially seen in PS19 mice, are well stained with M18 antibody. The morphological characteristics of the M18 staining in the entorhinal cortex at higher magnification indicate that astrocytes highly express LepRa (F). The boundary area of the hippocampal CA1 and cortex stained with M18, which indicates that expression of LepRa is restricted in the hippocampal area (G, lower area), but is extended neither to the adjacent white matter nor the cortex (G, upper area). K20 antibody, which recognizes all isoforms, weakly stains all brain regions beyond the hippocampus (H) (the upper side is the hilus of hippocampus and the down side is the thalamus). A high magnification image of the visual cortex shows that K20 stains both neurons (asterisks) and glial cells (arrowheads) (I). LepRb specific antibody, CH14014, weakly stains glial cells and neurons (J-L), but the staining intensities in CA3 regions from SD (J), HCD (K) and HCD + EX (L) are almost identical. This indicates that LepRb may weakly express on neurons and glial cells throughout all brain regions, although neurons in the basomedial hypothalamus express most highly (data not shown). Immunohistochemistry for pSTAT shows weak neuronal nuclear staining in pyramidal neurons in CA3 regions in SD (M), HCD (N) and HCD + EX (O). The similar tendency was also seen in hypothalamus in SD (P), HCD (Q) and HCD + EX (R). The staining intensity of HCD is weaker than SD or HCD + EX. Western blot for AMPK and its activated form pAMPK shows suppressed activity of AMPK in HCD. Meanwhile, HCD + EX shows upregulations of both AMPK expression and activity (S). 3V, 3rd ventricle. Scale bars, 100 μm in A–E; 10 μm in F, I–L; 50 μm in G, H, J–H, M–O.

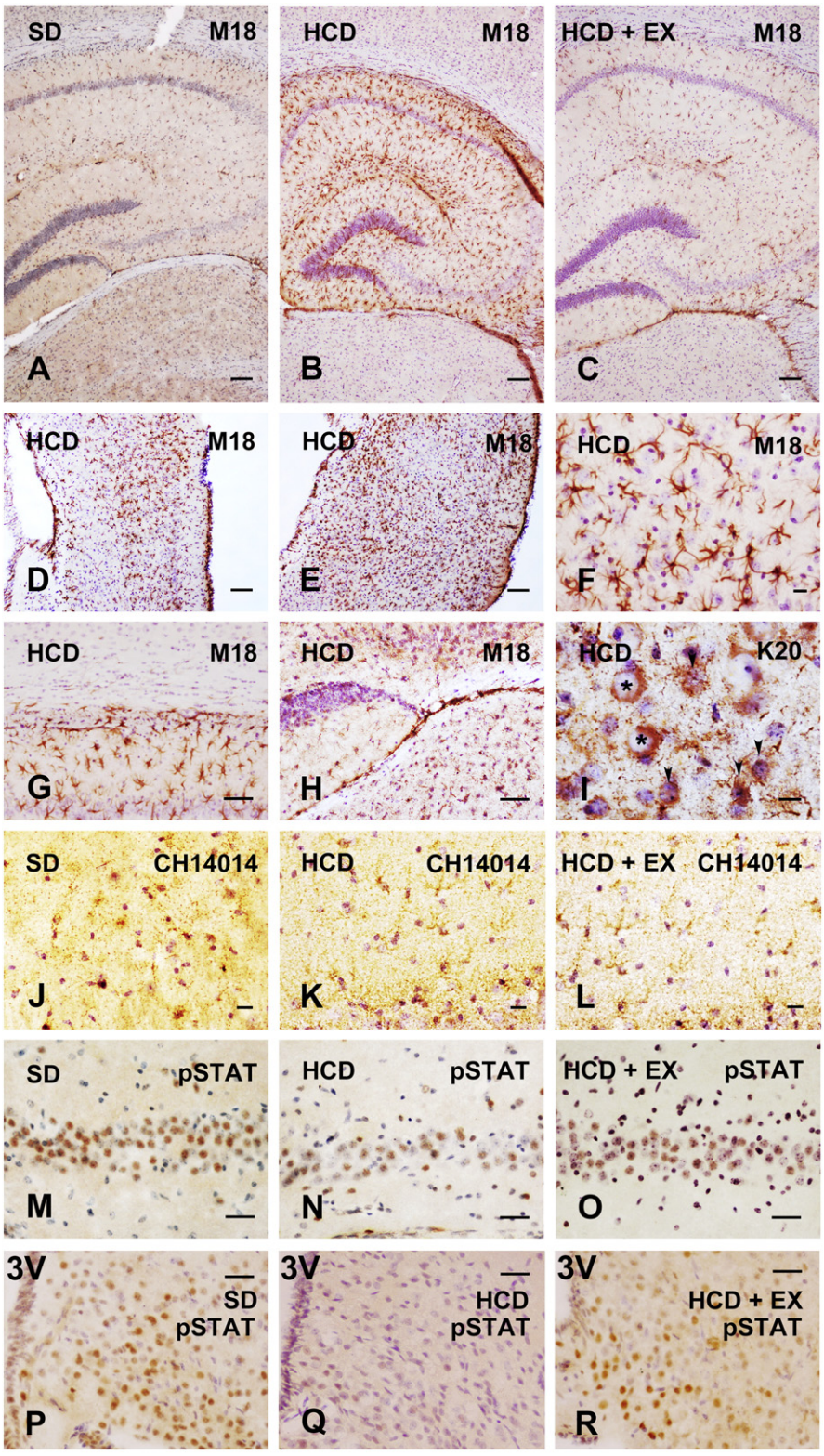
SD
M18
A
HCD
M18
B
HCD + EX
M18
C
HCD
M18
D
HCD
M18
E
HCD
M18
F
HCD
M18
G
HCD
M18
H
HCD
K20
I
SD
CH14014
J
HCD
CH14014
K
HCD + EX
CH14014
L
SD
pSTAT
M
HCD
pSTAT
N
HCD + EX
pSTAT
O
3V
SD
pSTAT
P
3V
HCD
pSTAT
Q
3V
HCD + EX
pSTAT
R

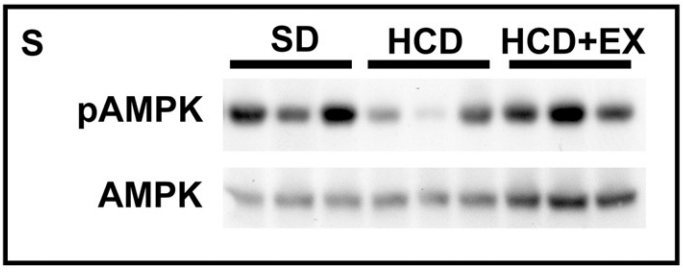
S
SD
HCD
HCD+EX
pAMPK
AMPK

expression of leptin receptors (LepRs) in the brain. LepRs are produced in several alternatively spliced forms that can be classified into three groups: long isoforms (LepRb), short isoforms (LepRa, c, d and f), and secreted isoforms (LepRe) (Lee et al., 1996; Wang et al., 1996). LepRb is the only full-length isoform, and was initially considered to be the functional receptor based on the finding that it has an extended intracellular domain containing various motifs required to interact with other proteins and subsequently activate signaling pathways (Tartaglia et al., 1995). Most of the effects of leptin on appetite and body weight are attributable to the central nervous system, especially the basomedial hypothalamus, where LepRb is highly expressed in neurons (Elmquist et al., 1998a, 1998b, 1999). We used three antibodies to distinguish LepR isoforms: M18, K20, and CH14014. M18 recognizes a portion of the LepR membrane that is juxtapositional to the cytoplasmic domain, and has the highest sensitivity for LepRa. It recognizes the other LepRs, but has less sensitivity for LepRc and LepRd, and the lowest sensitivity for LepRb (Hsuchou et al., 2009). K20 recognizes all isoforms except LepRe, and CH14014 is a LepRb-specific antibody. Low magnification images of brain tissue from PS19 mice fed HCD and stained with M18 antibody showed enhanced staining in the hippocampus (Fig. 5B) compared with PS19 mice fed SD (Fig. 5A) or HCD + EX (Fig. 5C). Higher magnification of the hippocampal CA1 area demonstrated selective staining with M18, which was not extended to the adjacent white matter or the cortices (Fig. 5G). Additionally, the entorhinal cortex (Fig. 5D) and the amygdala (Fig. 5E), where tau accumulation is commonly seen in PS19 mice, were highly stained with M18 antibody. The morphological characteristics of the M18 staining in the entorhinal cortex at higher magnification indicated that the LepR expression was in astrocytes (Fig. 5F). To investigate the LepR isoforms expressed in these astrocytes, RT-PCR on mRNA samples from primary cultured astrocytes derived from cortices, including the hippocampus was performed (Fig. 7A). Homogenate samples from the diencephalon (DC) showed clear bands of LepRa and b, and weak bands of LepRc, d, and e. Meanwhile, the primary cultured astrocytes showed clear bands of LepRa, a weaker band of LepRb, a faint band of LepRc, and trace bands of LepRd and e. Thus, the primary cultured astrocytes expressed mainly LepRa, while DC homogenate, which contained neurons, glial cells other than astrocytes, vessels, and other parenchyma, predominantly expressed LepRa and b. These findings corresponded to the immunohistochemical analysis for LepRs (Fig. 5). K20 weakly stained all brain regions beyond the hippocampus (Fig. 5H). A high magnification image of the visual cortex shows that K20 stained both neurons and glial cells (Fig. 5I). CH14014 weakly stained both glial cells and neurons (J–L), and the staining intensities in CA3 regions from SD (J), HCD (K), and HCD + EX (L) were almost identical. These results indicated that LepRb was widely expressed throughout the brain, including the hippocampus, neocortices, and hypothalamus (Mercer et al., 1996; Funahashi et al., 2003). Taken together, M18-stained astrocytes highly expressed LepRa, which might play a major role in these cells.

HCD induces leptin resistance both in hippocampal and hypothalamic neurons, but EX restores it

One of the most important signaling pathways medicated by LepRb is the signal transducer and activator of transcription-3 (STAT3) signaling pathway. Phosphorylation of STAT3 (pSTAT3) enables its nuclear translocation and promotes transcriptional effects. Thus, we performed immunochemistry to ascertain the prevalence of pSTAT3. Although an antibody specific to pSTAT3 stained nuclei of neurons in the hypothalamic nucleus (Figs. 5P–R), it also weakly stained hippocampal neurons (Figs. 5M–O). Meanwhile, there was no obvious glial staining, indicating that STAT3 and its downstream signaling might not operate in glial cells. Interestingly, the nuclei positive for pSTAT3 in the hippocampus region had similar staining in SD (Fig. 5M) and HCD + EX (Fig. 5O), but weaker staining in HCD (Fig. 5N), indicating that leptin resistance in HCD mice (Figs. 5N, Q) occurred not only in hypothalamic neurons (Figs. 5P–R), but also in hippocampal neurons (Figs. 5M–O). Because leptin can modulate AMP-activated protein kinase (AMPK) activity following binding to LepRb (Kola et al., 2006), we also performed a western blot for AMPK and its activated form, pAMPK. Although there was considerable sample-to-sample variation in the amount of pAMPK, it generally seemed decreased in samples from HCD mice. Interestingly, the AMPK expression was increased in HCD + EX, suggesting that EX might increase both the activation and expression of AMPK (Fig. 5S).

HCD enhances LepRa expression in astrocytes, but EX suppresses it

Astrocytes were activated and their LepRa expression was enhanced in the hippocampus of HCD PS19 mice. Therefore, we quantified the activation of astrocytes and their LepRa expression in double-stained hippocampal sections using an astrocyte-specific antibody for GFAP (Figs. 6A, D, G) and the M18 antibody (Figs. 6B, E, H). The staining clearly demonstrated astrocyte activation by intense GFAP staining, thickened cellular processes, and evidence of hypertrophy in the hippocampus in HCD mice (Fig. 6D). M18 staining was also stronger in astrocytes from HCD mice (Fig. 6E). Additionally, astrocyte proliferation was confirmed by counting the number of astrocytes (Figs. 6J, K). Merged images (Figs. 6C, F, I) demonstrated that not all GFAP-positive astrocytes were stained with M18. Activated astrocytes had increased M18 staining (Fig. 6F). This indicated that activation of astrocytes might induce and enhance LepRa expression. Quantitative analysis in hippocampal CA3 (Fig. 6J) and dentate gyrus (Fig. 6K) confirmed enhanced astrogliosis and LepRa expression in the hippocampus of HCD mice, and EX suppressed those changes (Figs. 6J, K).

Leptin induces Il-1β and TNF-α expression in primary cultured astrocytes via a LepRb-independent pathway

We speculated that astrocyte activation and enhanced astrocyte LepRa expression in HCD PS19 mice might play an important role in the enhanced tau pathology by activating inflammation. In addition to controlling appetite, it has been reported that leptin increases the expression of pro-inflammatory cytokines in some cell types, including IL-1β and TNF-α (Hosoi et al., 2000; Aleffi et al., 2005; Shen et al., 2005; Hekerman et al., 2007; Wong et al., 2007; Lafrance et al., 2010); it has also been reported that inflammation increases the levels of leptin and its receptors (Fernandez-Riejos et al., 2010; Gan et al., 2012). Because the expression of LepRa was enhanced in astrocytes in HCD-induced obese PS19 mice, we speculated hyperleptinemia induced inflammatory reactions in astrocytes with enhanced LepRa expression. To examine whether leptin induces pro-inflammatory cytokines in astrocytes, we conducted a leptin-load experiment in PCA. In this experiment, we used LepRb-deficient mice (*db*/*db*) and WT mice. Real time PCR analysis of TNF-α mRNA levels demonstrated a dose-dependent increase in both WT and *db*/*db* mice (Fig. 7D) in response to leptin. This clearly indicated that leptin likely induced TNF-α via LepRa and not via LepRb. Interestingly, IL-1β was increased only in *db*/*db* mice but not in WT mice (Fig. 7B). This suggests that the upregulation of short forms of LepRs (probably LepRa) induced by LepRb-deficiency in *db*/*db* mice might enhance IL-1β expression. Although C-C motif chemokine 2 (CCL2) (also called monocyte chemotactic protein-1 (MCP-1)), a small cytokine involved in neuroinflammatory processes, is highly expressed in astrocytes and neurons in the mouse brain (Ransohoff et al., 1993), leptin failed to alter mRNA levels of CCL2 (Fig. 7C).

Discussion

The most discriminative and important points in this study are that the HCD-induced obese tauopathy model mice we generated showed hyperleptinemia, but not obvious insulin resistance, and that EX ameliorated the hyperleptinemia without reducing body weight. These model mice and unique experimental conditions allowed us to explore the relationship between hyperleptinemia and changes related to enhanced tau

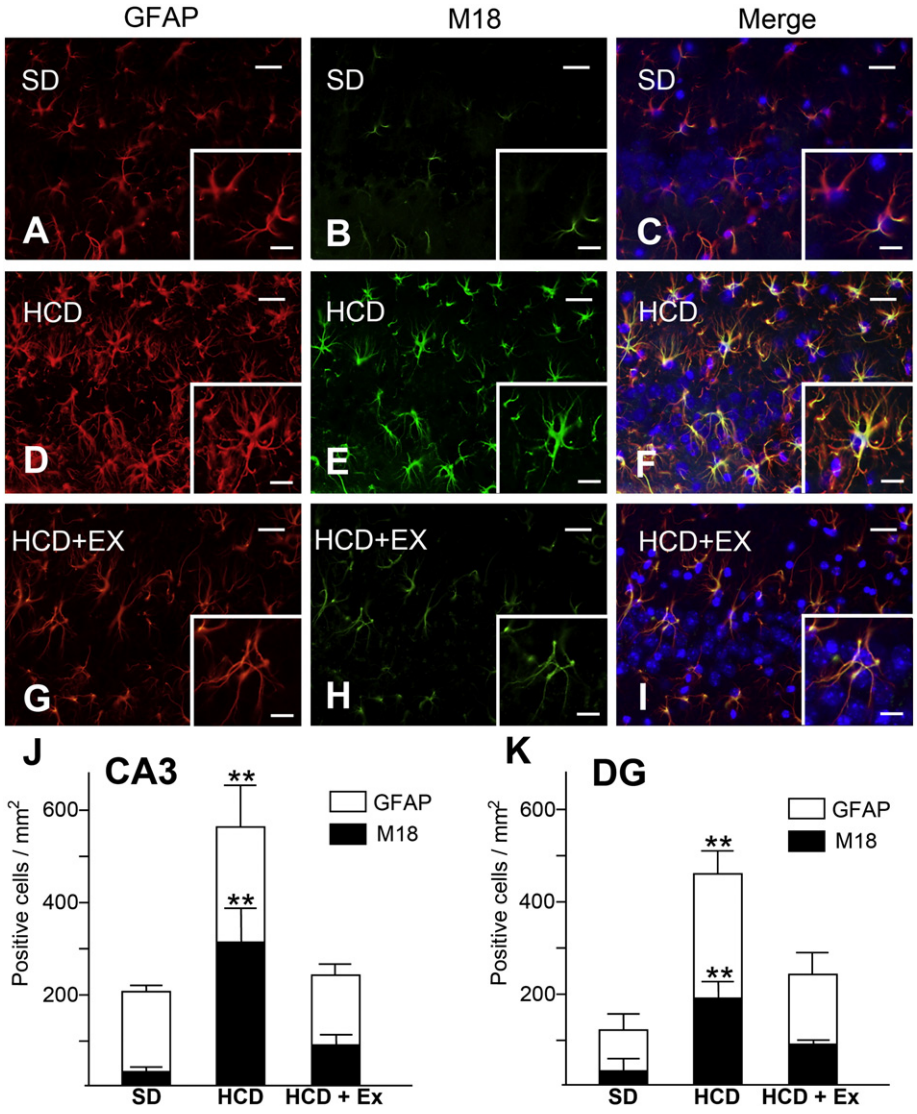

Fig. 6. HCD enhances, but EX attenuates astrogliosis and leptin receptor a (LepRa) expression in astrocytes. The immunostaining for GFAP (A, D, G) clearly demonstrates astroglial activation in HCD PS19 mice (D) compared with SD (A), and EX attenuates the astroglial activation (G). Immunostaining with M18 antibody (B, E, H), which preferentially recognizes LepRa, shows colocalization of GFAP and LepRa (C, F, I). The number of astrocytes positive for LepRa is increased in HCD (~50%) (F), but decreased in SD (~10%) (C) and HCD + EX (~30%) (I). Higher magnification images (insets) show that enhanced expression of LepRa is seen in more activated astrocytes. Quantitative analysis of cells positive for GFAP or LepRa indicates that significantly more GFAP- and LepRa-positive cells are found in the CA3 region (J) and the dentate gyrus (DG) (K) of the hippocampus (n = 4). Scale bars, 20 μm; 10 μm in insets. Error bars, 1 SE.

pathology, although it is impossible to completely exclude the possibilities that limited insulin signaling abnormality or other metabolic factors might play a role in enhancing tau pathology. The HCD we used here contains relatively lower fat and calories than the HCD used in a majority of diet-induced obesity studies; HCD usually contains around 35% fat, 60% cal from fat, and 550 cal/100 g. Meanwhile, HCD in this study contained 15.3% fat, 32% cal from fat and 415 cal/100 g. Therefore, the degree of obesity in this study was around 20% body weight gain, while that in other papers is usually more than 50% body weight gain, compared to the SD-fed mice. Additionally, the exercise quantity in HCD + EX in PS19 was about 10% less than that in WT mice (data not shown). This might be one of the reasons why EX did not reduce the body weight in HCD + EX PS19 mice. Recently, Leboucher et al. (2013) also demonstrated that obesity without insulin resistance enhanced hippocampal tau pathology in other tauopathy mouse model (THY-Tau22). This also indicates that mechanisms other than insulin signaling abnormalities play an important role in enhanced tau pathology induced by obesity. Because no reduction in the body weight was observed in the transgenic mice, the fat volume of the HCD + EX mice was presumably similar to that of the HCD PS19 mice. In fact, magnetic resonance spectroscopy and imaging of the body composition of the mice in vivo demonstrated that the voluntary exercise with the running wheel rarely changed the lean mass weight in obese MC4R-knockout mice and WT mice (Haskell-Luevano et al., 2009). EX activates LepR signaling pathways in HCD-induced obese mice (Flores et al., 2006; Ropelle et al., 2008), consequently lowering serum leptin levels (Krawczewski Carhuatanta et al., 2011). Krawczewski Carhuatanta et al. (2011) reported that HCD + EX mice showed a reduction in body weight with intracerebroventricular (ICV) leptin injection, but HCD-fed sedentary mice showed no reduction, even though the mice had the same fat mass as the HCD + EX mice. This indicated that EX improved HCD-induced leptin resistance independent of the increased adipose tissue (adiposity). These data support our speculation that EX might reduce leptin concentration by improving leptin resistance and not by reducing adipose tissue. Meanwhile, it has been reported that EX has beneficial effects on neurodegeneration and inflammation in both the presence and absence of obesity (Adlard et al., 2005; Cotman et al., 2007; Bradley et al., 2008; Balducci et al., 2010). We found no significant beneficial effects of EX on tau pathology (Supplemental Figs. 1A, B), tau insolubility (Supplemental Fig. 1F), microglial activation (Supplemental Figs. 1C, D), astrocytic LepRa expression (Supplemental Fig. 1E) or metabolic parameters (Supplemental Table 1) in SD-fed PS19 mice, although western blotting showed that ERK1/2

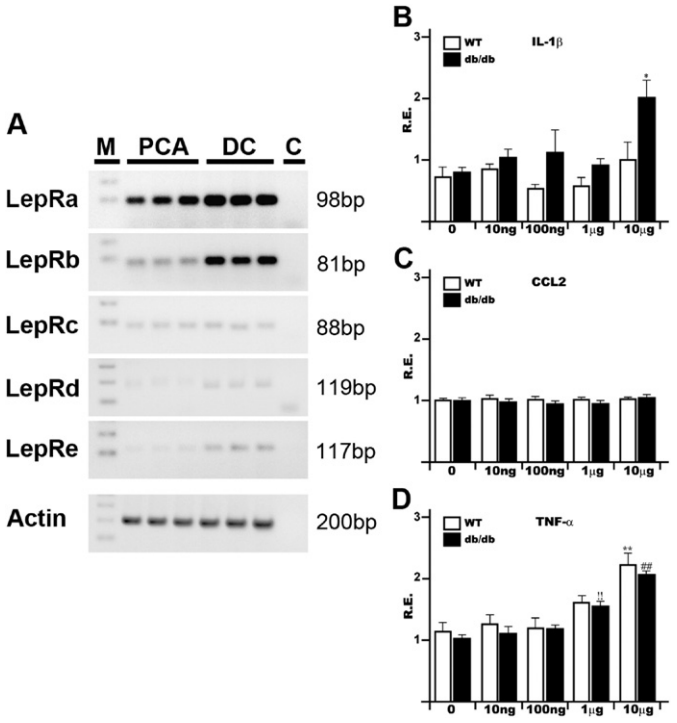

Fig. 7. The mRNA levels of leptin receptor isoforms and the effects of leptin on primary cultured astrocytes (PCA). RT-PCR analysis shows that cortical primary cultured astrocytes (PCA) from wild type mice predominantly express LepRa (98 bp), slightly express LepRb (81 bp), and barely express LepRc (88 bp), LepRd (119 bp) or LepRe (117 bp). Meanwhile, the level of LepRb is comparable to LepRa in mRNA extracted from the diencephalon (DC) homogenates (A). The same RT-PCR procedure without template was done for the control experiment (C). Real time PCR demonstrates that leptin significantly increases the mRNA expression levels of TNF-α in a dose-dependent manner in both wild type (WT) astrocytes and LepRb-deficient mouse (*db*/*db*) astrocytes (D) but not the level of CCL2 (C) ($n = 5$). Interestingly, high concentrations of leptin induce IL-1β only in only *db*/*db* mouse astrocytes (B). (A) M: 100 pb ladders; C: No template. (B) *: $p < 0.03$ to 0 ng/ml. (D) **: $p < 0.01$ to 0 ng/ml and 100 ng/ml; $p < 0.03$ to 10 ng/ml. !!: $p < 0.01$ to all other concentrations. ##: $p < 0.01$ to all other concentrations. Error bars, 1 SE.

phosphorylation was suppressed (Supplemental Fig. 1F). This indicated that EX itself had fewer direct effects on tau pathology and glial activation, therefore, we speculated that the hyperleptinemia induced by HCD and the suppression of that hyperleptinemia by EX might be the main mechanism alternating tau pathology and glial activation, although we cannot exclude the possibility that other pathomechanisms related to obesity and EX play a role in the pathological changes. Additionally, because we did not use cages with the blocked running wheel as controls, environmental differences including cage circumstances might have an affect on the pathology and metabolic changes. Thus, further, more precise experiments are required to show the roles of persistent hyperleptinemia in tau pathology and neurodegeneration. Although the evaluation of HCD effects on cognitive and behavioral functions must be important as same as pathological changes, we did not analyze those, because old PS19 mice showed motor symptoms (paralysis). Recently, Knight et al. (2014) reported that high-fat diet induced memory impairment without enhanced amyloid or tau pathology in 3xTgAD mice (APP_Swe, $PS1_{M146}$, TAU_{P301L}). This indicates that obesity itself might affect the cognitive functions without enhanced AD pathological changes.

Leptin is primarily thought to be an anti-obesity hormone because its main physiological function is to prevent obesity by regulating the balance between food intake and energy expenditure. This activity occurs in the basomedial hypothalamus. Although hypothalamic nuclei express LepRb in the greatest density, other LepRs are abundantly expressed in neurons and glial cells throughout the brain (Mercer et al., 1996; Funahashi et al., 2003), suggesting that leptin might play some role in physiological or pathological processes in the brain besides balancing food intake and energy expenditure. In fact, beneficial effects of leptin on neuronal survival have been reported (Signore et al., 2008; Folch et al., 2012). Leptin mitigates tau phosphorylation in cultured neuronal cells (Greco et al., 2008), and continuous intraperitoneal injection of leptin in amyloidogenic transgenic mice (CRND8) reduced amyloid burden and tau phosphorylation in vivo (Greco et al., 2010). Additionally, the pro-inflammatory effects of leptin have been shown in a variety of different cell types (Hosoi et al., 2000; Aleffi et al., 2005; Shen et al., 2005; Hekerman et al., 2007; Wong et al., 2007; Lafrance et al., 2010). Hyperleptinemia induced by peritoneal dialysis with glucose-containing fluid increased expression of pro-inflammatory cytokines including TNF-α and IL-6 in visceral adipose tissue in mice. Interestingly, these effects were stronger in obese, LepRb-deficient *db*/*db* mice compared with their non-obese littermates (*db*/*m*), characterized by an upregulation of LepRa expression (Leung et al., 2012). Chronic ICV administration of leptin activated astrocytes and enhanced GFAP and vimentin expression in adult male rats. Additionally, obese adult male rats with hyperleptinemia caused by neonatal overnutrition showed similar changes in glial structural proteins (Garcia-Caceres et al., 2011). In our study, HCD-induced obesity also caused astrocytic activation with enhanced GFAP expression. These results indicate that high levels of circulating leptin induced by obesity might act on astrocytes similarly to chronic ICV administration of leptin, suggesting that the effects of leptin on astrocytes might not be suppressed when so-called "leptin resistance" occurs, in which leptin effects on neurons and neuronal circuits are down-regulated (Fig. 8).

Because there are few studies about LepRa and its functions, the function of LepRa in astrocytes is not clear, but analysis of astrocytic LepR knockout mice (ALKO) provides some indications about LepRa function in astrocytes. Interestingly, ALKO showed less hyperleptinemia and GFAP expression than WT mice when HCD was supplied, although the differences between ALKO and WT mice were not seen when SD was supplied (Jayaram et al., 2013). They speculated that in the case of prolonged HCD, astrocytic LepRs became highly reactive to circulating concentrations of leptin, followed by astroglial activation and proinflammatory cytokine secretion, which eventually led to neuroinflammation. Neuroinflammation reduces sensitivity of neurons to leptin (leptin resistance), enhancing hyperleptinemia even more (Jayaram et al., 2013). This speculation is based on a series of pathological events in the hypothalamus that explain the impaired leptin signaling. Fig. 8 shows a model of how hyperleptinemia acts in the hypothalamus and hippocampus in the obese tau mouse model. Hyperleptinemia caused by HCD-induced obesity reduces the leptin sensitivity of neurons in the hypothalamus, further increasing hyperleptinemia while enhancing the sensitivity of leptin in astrocytes (astrogliosis and enhanced expression of LepRa) and accelerating inflammatory responses, including the secretion of pro-inflammatory cytokines and microglial activation. Thus, the enhanced neuroinflammation induced by hyperleptinemia could accelerate tau pathology and neurodegeneration with tau hyperphosphorylation. Moreover, downregulation of leptin sensitivity in hippocampal neurons (leptin resistance) simultaneously might reduce the suppressive effects of tau phosphorylation caused by leptin (Greco et al., 2009) and the neuroprotective effects of leptin (Tezapsidis et al., 2009). Our findings do not mean that persistent hyperleptinemia directly initiates tau pathology, but they do indicate that persistent hyperleptinemia could accelerate any existing tau pathology.

In conclusion, we showed that persistent hyperleptinemia caused by HCD-induced obesity enhanced astrogliosis, increased astrocytic LepRa expression, and increased tau pathology in a tauopathy mouse model. These pathological deteriorations were restored by EX, which improved leptin sensitivity. The effects of obesity on tau pathology are not easy to define because they include the effects of obesity itself and the effects of diseases caused by obesity. Although it is inappropriate to simplistically apply the results in this study to humans, hyperleptinemia might be

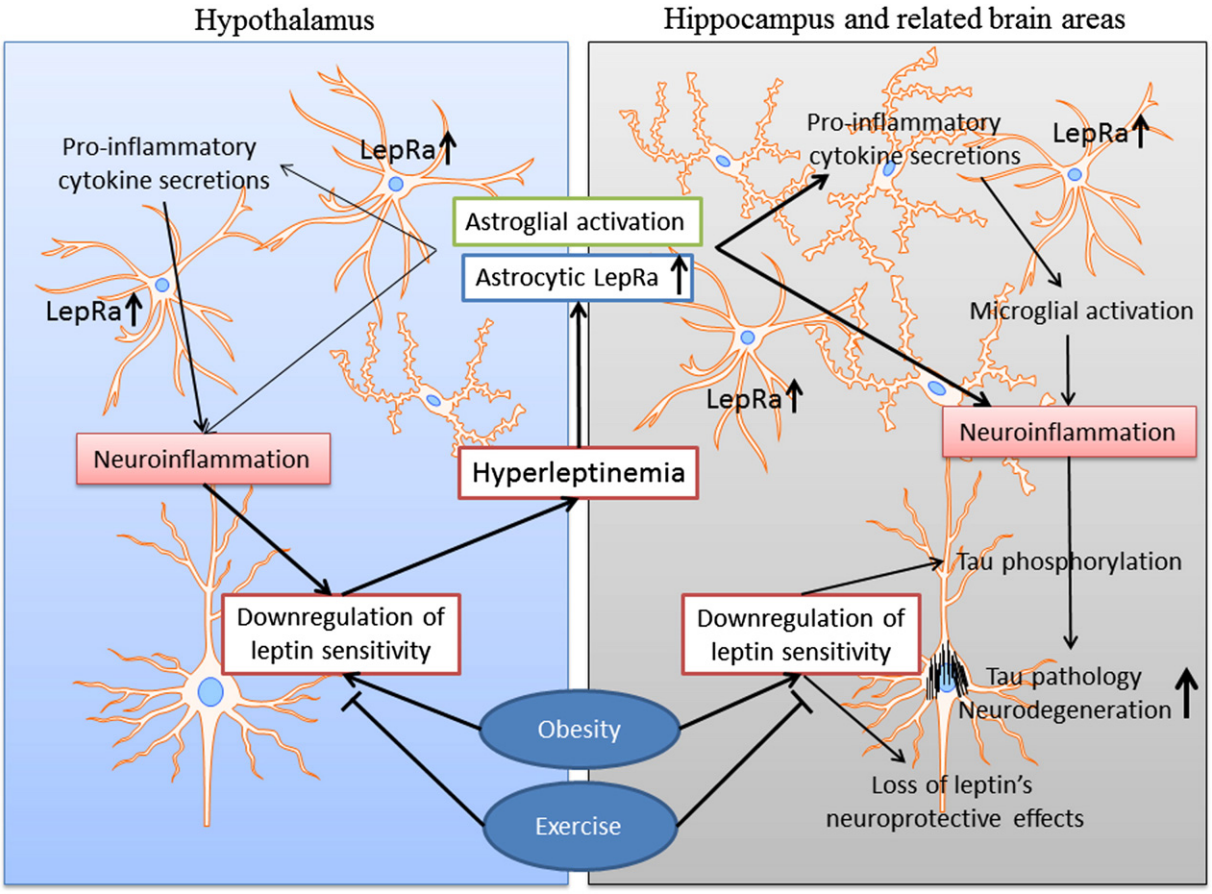

Fig. 8. Schematic representation of effects of HCD-induced hyperleptinemia on glial activation, tau pathology and neurodegeneration in PS19 mice. HCD induces obesity and the downregulation of leptin sensitivity (leptin resistance), leading to hyperleptinemia. Astrocyte activation and LepRa expression in the hypothalamus caused by chronic hyperleptinemia further reduces leptin sensitivity. Simultaneously, hyperleptinemia accelerates neuroinflammation, including astroglial activation and microglial activation, and pro-inflammatory cytokine secretion in the hippocampus and related brain areas where tau pathology and neurodegeneration commonly appear. Additionally, the downregulation of leptin sensitivity decreases neuroprotective effects of leptin. Meanwhile, EX improves the leptin sensitivity.

a key pathomechanism that links the effects of obesity and exercise with AD.

Supplementary data to this article can be found online at http://dx.doi.org/10.1016/j.nbd.2014.08.015.

Acknowledgments

This work was supported by funding from Grant-in-Aid for Scientific Research (C), and Takeda Science Foundation to Y.Y. The authors declare that the research was carried out in the absence of any commercial or financial relationships that might be construed as a potential conflict of interest.

References

Adlard, P.A., Perreau, V.M., Pop, V., Cotman, C.W., 2005. Voluntary exercise decreases amyloid load in a transgenic model of Alzheimer's disease. J. Neurosci. 25, 4217–4221.
Akiyama, H., et al., 2000. Inflammation and Alzheimer's disease. Neurobiol. Aging 21, 383–421.
Aleffi, S., Petrai, I., Bertolani, C., Parola, M., Colombatto, S., Novo, E., Vizzutti, F., Anania, F.A., Milani, S., Rombouts, K., Laffi, G., Pinzani, M., Marra, F., 2005. Upregulation of proinflammatory and proangiogenic cytokines by leptin in human hepatic stellate cells. Hepatology 42, 1339–1348.
Balducci, S., Zanuso, S., Nicolucci, A., Fernando, F., Cavallo, S., Cardelli, P., Fallucca, S., Alessi, E., Letizia, C., Jimenez, A., Fallucca, F., Pugliese, G., 2010. Anti-inflammatory effect of exercise training in subjects with type 2 diabetes and the metabolic syndrome is dependent on exercise modalities and independent of weight loss. Nutr. Metab. Cardiovasc. Dis. 20, 608–617.
Borchelt, D.R., Davis, J., Fischer, M., Lee, M.K., Slunt, H.H., Ratovitsky, T., Regard, J., Copeland, N.G., Jenkins, N.A., Sisodia, S.S., Price, D.L., 1996. A vector for expressing foreign genes in the brains and hearts of transgenic mice. Genet. Anal. 13, 159–163.
Bradley, R.L., Jeon, J.Y., Liu, F.F., Maratos-Flier, E., 2008. Voluntary exercise improves insulin sensitivity and adipose tissue inflammation in diet-induced obese mice. Am. J. Physiol. Endocrinol. Metab. 295, E586–E594.
Chen, F., 2012. JNK-induced apoptosis, compensatory growth, and cancer stem cells. Cancer Res. 72, 379–386.
Cotman, C.W., Berchtold, N.C., Christie, L.A., 2007. Exercise builds brain health: key roles of growth factor cascades and inflammation. Trends Neurosci. 30, 464–472.
Elmquist, J.K., Maratos-Flier, E., Saper, C.B., Flier, J.S., 1998a. Unraveling the central nervous system pathways underlying responses to leptin. Nat. Neurosci. 1, 445–450.
Elmquist, J.K., Bjorbaek, C., Ahima, R.S., Flier, J.S., Saper, C.B., 1998b. Distributions of leptin receptor mRNA isoforms in the rat brain. J. Comp. Neurol. 395, 535–547.
Elmquist, J.K., Elias, C.F., Saper, C.B., 1999. From lesions to leptin: hypothalamic control of food intake and body weight. Neuron 22, 221–232.
Fernandez-Riejos, P., Najib, S., Santos-Alvarez, J., Martin-Romero, C., Perez-Perez, A., Gonzalez-Yanes, C., Sanchez-Margalet, V., 2010. Role of leptin in the activation of immune cells. Mediat. Inflamm. 2010, 568343.
Finucane, M.M., Stevens, G.A., Cowan, M.J., Danaei, G., Lin, J.K., Paciorek, C.J., Singh, G.M., Gutierrez, H.R., Lu, Y., Bahalim, A.N., Farzadfar, F., Riley, L.M., Ezzati, M., Global Burden of Metabolic Risk Factors of Chronic Diseases Collaborating G, 2011. National, regional, and global trends in body-mass index since 1980: systematic analysis of health examination surveys and epidemiological studies with 960 country-years and 9.1 million participants. Lancet 377, 557–567.
Flores, M.B., Fernandes, M.F., Ropelle, E.R., Faria, M.C., Ueno, M., Velloso, L.A., Saad, M.J., Carvalheira, J.B., 2006. Exercise improves insulin and leptin sensitivity in hypothalamus of Wistar rats. Diabetes 55, 2554–2561.
Folch, J., Pedros, I., Patraca, I., Sureda, F., Junyent, F., Beas-Zarate, C., Verdaguer, E., Pallas, M., Auladell, C., Camins, A., 2012. Neuroprotective and anti-ageing role of leptin. J. Mol. Endocrinol. 49, R149–R156.
Fukutani, Y., Cairns, N.J., Shiozawa, M., Sasaki, K., Sudo, S., Isaki, K., Lantos, P.L., 2000. Neuronal loss and neurofibrillary degeneration in the hippocampal cortex in late-onset sporadic Alzheimer's disease. Psychiatry Clin. Neurosci. 54, 523–529.
Funahashi, H., Yada, T., Suzuki, R., Shioda, S., 2003. Distribution, function, and properties of leptin receptors in the brain. Int. Rev. Cytol. 224, 1–27.
Gan, L., Guo, K., Cremona, M.L., McGraw, T.E., Leibel, R.L., Zhang, Y., 2012. TNF-alpha upregulates protein level and cell surface expression of the leptin receptor by stimulating its export via a PKC-dependent mechanism. Endocrinology 153, 5821–5833.

Garcia-Caceres, C., Fuente-Martin, E., Burgos-Ramos, E., Granado, M., Frago, L.M., Barrios, V., Horvath, T., Argente, J., Chowen, J.A., 2011. Differential acute and chronic effects of leptin on hypothalamic astrocyte morphology and synaptic protein levels. Endocrinology 152, 1809–1818.

Gleeson, M., Bishop, N.C., Stensel, D.J., Lindley, M.R., Mastana, S.S., Nimmo, M.A., 2011. The anti-inflammatory effects of exercise: mechanisms and implications for the prevention and treatment of disease. Nat. Rev. Immunol. 11, 607–615.

Greco, S.J., Sarkar, S., Johnston, J.M., Zhu, X., Su, B., Casadesus, G., Ashford, J.W., Smith, M.A., Tezapsidis, N., 2008. Leptin reduces Alzheimer's disease-related tau phosphorylation in neuronal cells. Biochem. Biophys. Res. Commun. 376, 536–541.

Greco, S.J., Sarkar, S., Casadesus, G., Zhu, X., Smith, M.A., Ashford, J.W., Johnston, J.M., Tezapsidis, N., 2009. Leptin inhibits glycogen synthase kinase-3beta to prevent tau phosphorylation in neuronal cells. Neurosci. Lett. 455, 191–194.

Greco, S.J., Bryan, K.J., Sarkar, S., Zhu, X., Smith, M.A., Ashford, J.W., Johnston, J.M., Tezapsidis, N., Casadesus, G., 2010. Leptin reduces pathology and improves memory in a transgenic mouse model of Alzheimer's disease. J. Alzheimers Dis. 19, 1155–1167.

Gustafson, D.R., Backman, K., Waern, M., Ostling, S., Guo, X., Zandi, P., Mielke, M.M., Bengtsson, C., Skoog, I., 2009. Adiposity indicators and dementia over 32 years in Sweden. Neurology 73, 1559–1566.

Haskell-Luevano, C., Schaub, J.W., Andreasen, A., Haskell, K.R., Moore, M.C., Koerper, L.M., Rouzaud, F., Baker, H.V., Millard, W.J., Walter, G., Litherland, S.A., Xiang, Z., 2009. Voluntary exercise prevents the obese and diabetic metabolic syndrome of the melanocortin-4 receptor knockout mouse. FASEB J. 23, 642–655.

Hekerman, P., Zeidler, J., Korfmacher, S., Bamberg-Lemper, S., Knobelspies, H., Zabeau, L., Tavernier, J., Becker, W., 2007. Leptin induces inflammation-related genes in RINm5F insulinoma cells. BMC Mol. Biol. 8, 41.

Hirosumi, J., Tuncman, G., Chang, L., Gorgun, C.Z., Uysal, K.T., Maeda, K., Karin, M., Hotamisligil, G.S., 2002. A central role for JNK in obesity and insulin resistance. Nature 420, 333–336.

Hosoi, T., Okuma, Y., Nomura, Y., 2000. Expression of leptin receptors and induction of IL-1beta transcript in glial cells. Biochem. Biophys. Res. Commun. 273, 312–315.

Hotamisligil, G.S., Erbay, E., 2008. Nutrient sensing and inflammation in metabolic diseases. Nat. Rev. Immunol. 8, 923–934.

Hsuchou, H., He, Y., Kastin, A.J., Tu, H., Markadakis, E.N., Rogers, R.C., Fossier, P.B., Pan, W., 2009. Obesity induces functional astrocytic leptin receptors in hypothalamus. Brain 132, 889–902.

Jayaram, B., Pan, W., Wang, Y., Hsuchou, H., Mace, A., Cornelissen-Guillaume, G.G., Mishra, P.K., Koza, R.A., Kastin, A.J., 2013. Astrocytic leptin-receptor knockout mice show partial rescue of leptin resistance in diet-induced obesity. J. Appl. Physiol. 114, 734–741.

Kivipelto, M., Ngandu, T., Fratiglioni, L., Viitanen, M., Kareholt, I., Winblad, B., Helkala, E.L., Tuomilehto, J., Soininen, H., Nissinen, A., 2005. Obesity and vascular risk factors at midlife and the risk of dementia and Alzheimer disease. Arch. Neurol. 62, 1556–1560.

Knight, E.M., Martins, I.V., Gumusgoz, S., Allan, S.M., Lawrence, C.B., 2014. High-fat diet-induced memory impairment in triple-transgenic Alzheimer's disease (3xTgAD) mice is independent of changes in amyloid and tau pathology. Neurobiol. Aging 35, 1821–1832.

Kola, B., Boscaro, M., Rutter, G.A., Grossman, A.B., Korbonits, M., 2006. Expanding role of AMPK in endocrinology. Trends Endocrinol. Metab. 17, 205–215.

Krawczewski Carhuatanta, K.A., Demuro, G., Tschop, M.H., Pfluger, P.T., Benoit, S.C., Obici, S., 2011. Voluntary exercise improves high-fat diet-induced leptin resistance independent of adiposity. Endocrinology 152, 2655–2664.

Lafrance, V., Inoue, W., Kan, B., Luheshi, G.N., 2010. Leptin modulates cell morphology and cytokine release in microglia. Brain Behav. Immun. 24, 358–365.

Leboucher, A., Laurent, C., Fernandez-Gomez, F.J., Burnouf, S., Troquier, L., Eddarkaoui, S., Demeyer, D., Caillierez, R., Zommer, N., Vallez, E., Bantubungi, K., Breton, C., Pigny, P., Buee-Scherrer, V., Staels, B., Hamdane, M., Tailleux, A., Buee, L., Blum, D., 2013. Detrimental effects of diet-induced obesity on tau pathology are independent of insulin resistance in tau transgenic mice. Diabetes 62, 1681–1688.

Lee, G.H., Proenca, R., Montez, J.M., Carroll, K.M., Darvishzadeh, J.G., Lee, J.I., Friedman, J.M., 1996. Abnormal splicing of the leptin receptor in diabetic mice. Nature 379, 632–635.

Leung, J.C., Chan, L.Y., Lam, M.F., Tang, S.C., Chow, C.W., Lim, A.I., Lai, K.N., 2012. The role of leptin and its short-form receptor in inflammation in db/db mice infused with peritoneal dialysis fluid. Nephrol. Dial. Transplant. Off. Publ. Eur. Dial. Transpl. Assoc. - Eur. Ren. Assoc. 27, 3119–3129.

Li, N.C., Lee, A., Whitmer, R.A., Kivipelto, M., Lawler, E., Kazis, L.E., Wolozin, B., 2010. Use of angiotensin receptor blockers and risk of dementia in a predominantly male population: prospective cohort analysis. BMJ 340 (b5465-b5465).

Li, C., Zhao, R., Gao, K., Wei, Z., Yin, M.Y., Lau, L.T., Chui, D., Hoi Yu, A.C., 2011. Astrocytes: implications for neuroinflammatory pathogenesis of Alzheimer's disease. Curr. Alzheimer Res. 8, 67–80.

McArdle, M.A., Finucane, O.M., Connaughton, R.M., McMorrow, A.M., Roche, H.M., 2013. Mechanisms of obesity-induced inflammation and insulin resistance: insights into the emerging role of nutritional strategies. Front. Endocrinol. 4, 52.

McCarthy, K.D., de Vellis, J., 1980. Preparation of separate astroglial and oligodendroglial cell cultures from rat cerebral tissue. J. Cell Biol. 85, 890–902.

Mercer, J.G., Hoggard, N., Williams, L.M., Lawrence, C.B., Hannah, L.T., Trayhurn, P., 1996. Localization of leptin receptor mRNA and the long form splice variant (Ob-Rb) in mouse hypothalamus and adjacent brain regions by in situ hybridization. FEBS Lett. 387, 113–116.

Petersen, A.M., Pedersen, B.K., 2005. The anti-inflammatory effect of exercise. J. Appl. Physiol. 98, 1154–1162.

Profenno, L.A., Porsteinsson, A.P., Faraone, S.V., 2010. Meta-analysis of Alzheimer's disease risk with obesity, diabetes, and related disorders. Biol. Psychiatry 67, 505–512.

Ransohoff, R.M., Hamilton, T.A., Tani, M., Stoler, M.H., Shick, H.E., Major, J.A., Estes, M.L., Thomas, D.M., Tuohy, V.K., 1993. Astrocyte expression of mRNA encoding cytokines IP-10 and JE/MCP-1 in experimental autoimmune encephalomyelitis. FASEB J. 7, 592–600.

Ropelle, E.R., Fernandes, M.F., Flores, M.B., Ueno, M., Rocco, S., Marin, R., Cintra, D.E., Velloso, L.A., Franchini, K.G., Saad, M.J., Carvalheira, J.B., 2008. Central exercise action increases the AMPK and mTOR response to leptin. PLoS ONE 3, e3856.

Shen, J., Sakaida, I., Uchida, K., Terai, S., Okita, K., 2005. Leptin enhances TNF-alpha production via p38 and JNK MAPK in LPS-stimulated Kupffer cells. Life Sci. 77, 1502–1515.

Signore, A.P., Zhang, F., Weng, Z., Gao, Y., Chen, J., 2008. Leptin neuroprotection in the CNS: mechanisms and therapeutic potentials. J. Neurochem. 106, 1977–1990.

Tartaglia, L.A., Dembski, M., Weng, X., Deng, N., Culpepper, J., Devos, R., Richards, G.J., Campfield, L.A., Clark, F.T., Deeds, J., Muir, C., Sanker, S., Moriarty, A., Moore, K.J., Smutko, J.S., Mays, G.G., Wool, E.A., Monroe, C.A., Tepper, R.I., 1995. Identification and expression cloning of a leptin receptor, OB-R. Cell 83, 1263–1271.

Tezapsidis, N., Johnston, J.M., Smith, M.A., Ashford, J.W., Casadesus, G., Robakis, N.K., Wolozin, B., Perry, G., Zhu, X., Greco, S.J., Sarkar, S., 2009. Leptin: a novel therapeutic strategy for Alzheimer's disease. J. Alzheimers Dis. 16, 731–740.

van Greevenbroek, M.M., Schalkwijk, C.G., Stehouwer, C.D., 2013. Obesity-associated low-grade inflammation in type 2 diabetes mellitus: causes and consequences. Neth. J. Med. 71, 174–187.

Wang, M.Y., Zhou, Y.T., Newgard, C.B., Unger, R.H., 1996. A novel leptin receptor isoform in rat. FEBS Lett. 392, 87–90.

Whitmer, R.A., Gunderson, E.P., Quesenberry Jr., C.P., Zhou, J., Yaffe, K., 2007. Body mass index in midlife and risk of Alzheimer disease and vascular dementia. Curr. Alzheimer Res. 4, 103–109.

Wong, C.K., Cheung, P.F., Lam, C.W., 2007. Leptin-mediated cytokine release and migration of eosinophils: implications for immunopathophysiology of allergic inflammation. Eur. J. Immunol. 37, 2337–2348.

Yoshiyama, Y., Higuchi, M., Zhang, B., Huang, S.M., Iwata, N., Saido, T.C., Maeda, J., Suhara, T., Trojanowski, J.Q., Lee, V.M., 2007. Synapse loss and microglial activation precede tangles in a P301S tauopathy mouse model. Neuron 53, 337–351.

Yoshiyama, Y., Kojima, A., Ishikawa, C., Arai, K., 2010. Anti-inflammatory action of donepezil ameliorates tau pathology, synaptic loss, and neurodegeneration in a tauopathy mouse model. J. Alzheimers Dis. 22, 295–306.

Yoshiyama, Y., Kojima, A., Itoh, K., Uchiyama, T., Arai, K., 2012. Anticholinergics boost the pathological process of neurodegeneration with increased inflammation in a tauopathy mouse model. Neurobiol. Dis. 45, 329–336.

Yoshiyama, Y., Lee, V.M., Trojanowski, J.Q., 2013. Therapeutic strategies for tau mediated neurodegeneration. J. Neurol. Neurosurg. Psychiatry 84, 784–795.